

# Selective electrochemical degradation of bottlebrush elastomers

Kaitlin R. Albanese<sup>1</sup> | Parker T. Morris<sup>1,2</sup> | Brian Roehrich<sup>2</sup> |  
Javier Read de Alaniz<sup>2</sup> | Craig J. Hawker<sup>1,3</sup> | Christopher M. Bates<sup>1,3</sup> 

<sup>1</sup>Materials Research Laboratory, University of California, Santa Barbara, Santa Barbara, California, USA

<sup>2</sup>Department of Chemistry & Biochemistry, University of California, Santa Barbara, Santa Barbara, California, USA

<sup>3</sup>Materials Department, University of California, Santa Barbara, Santa Barbara, California, USA

## Correspondence

Christopher M. Bates, Materials Research Laboratory, University of California, Santa Barbara, Santa Barbara, CA 93106, USA.  
Email: [cbates@ucsb.edu](mailto:cbates@ucsb.edu)

Javier Read de Alaniz, Department of Chemistry & Biochemistry, University of California, Santa Barbara, Santa Barbara, CA 93106, USA.  
Email: [javier@chem.ucsb.edu](mailto:javier@chem.ucsb.edu)

Craig J. Hawker, Materials Research Laboratory, University of California, Santa Barbara, Santa Barbara, CA 93106, USA.  
Email: [hawker@mrl.ucsb.edu](mailto:hawker@mrl.ucsb.edu)

## Funding information

National Science Foundation,  
Grant/Award Numbers: DMR-1933487,  
DMR-2308708

## Abstract

We introduce a simple synthetic strategy to selectively degrade bottlebrush networks derived from well-defined poly(4-methylcaprolactone) (P4MCL) bottlebrush polymers. Functionalization of the hydroxyl groups present at the terminal ends of P4MCL side chains with  $\alpha$ -lipoic acid resulted in bottlebrush polymers having a range of molecular weights ( $M_n = 45\text{--}2200 \text{ kg mol}^{-1}$ ) and a tunable number of reactive dithiolane chain ends. These functionalized chain ends act as efficient crosslinkers due to radical ring-opening of the dithiolane rings under UV light. The resulting redox-active disulfide crosslinks enable mild electrochemical or chemical degradation of the S–S crosslinks to regenerate the starting bottlebrush polymer. P4MCL side chains and the disulfides can be degraded simultaneously using harsher reducing conditions. This combination of bottlebrush architecture with facile disulfide crosslinking presents a versatile platform for preparing highly tunable elastomers that undergo controlled degradation under mild conditions.

## KEY WORDS

bottlebrush network, degradable, electrochemical degradation, lipoic acid

## 1 | INTRODUCTION

Bottlebrush polymers and networks derived therefrom have attracted significant attention as super-soft materials ( $G' \leq 100 \text{ kPa}$ ) with highly tunable physical properties governed by their densely grafted side chains.<sup>1–8</sup> The bottlebrush architecture endows unique material properties directed by (i) a high density of side chains and chain ends, (ii) suppressed chain entanglements, and (iii) an elongated backbone arising from side-chain repulsion. These unique characteristics have facilitated the development of bottlebrush polymers with innovative applications that are not possible with linear polymers.<sup>1,8–12</sup>

We recently reported an example of degradable bottlebrush elastomers based on poly(dimethylsiloxane) (PDMS)-functionalized  $\alpha$ -lipoic acid (LA) building blocks which give rise to a disulfide-containing backbone that can be degraded under reductive conditions.<sup>7</sup> Zheng et al. designed similar silicone bottlebrush networks for thermally conductive materials leveraging LA as a dynamic backbone for reprocessing.<sup>13</sup> However, these networks required high temperatures ( $< 120^\circ\text{C}$ ) and long reaction times (4 h) for radical ring-opening polymerization (rROP) to occur, which plateaued at  $\sim 50\%$  monomer conversion. The Feringa group also reported LA functionalized PDMS networks constructed through

photoinitiated rROP of LA crosslinks.<sup>14</sup> In this case, PDMS functionalization afforded only 80% coupling efficiency to the LA monomer with additional examples of degradable bottlebrushes relying on radical-based polymerization methods to construct the bottlebrush backbone.<sup>15–20</sup> For example, Roth and coworkers synthesized water-soluble bottlebrush polymers through atom-transfer radical polymerization (ATRP), incorporating dibenzo[c, e]oxepin-5(7H)-thione copolymers into the side-chains.<sup>17</sup> While several significant advancements in degradable bottlebrush elastomers have been achieved, many proposed radical methods are limited to lower molecular weight bottlebrushes.

Here, we introduce a versatile synthetic strategy to form bottlebrush networks from well-defined bottlebrush macromonomers which enables the synthesis of bottlebrush polymers with a wide range of molecular weights ( $M_n = 45\text{--}2200 \text{ kg mol}^{-1}$ ) (Figure 1).<sup>1–4,16,21,22</sup> The resulting chain ends of the molecular bottlebrushes are then readily functionalized through simple coupling with  $\alpha$ -lipoic acid (LA)—a dithiolane known to undergo rROP with different stimuli such as heat<sup>7,23–29</sup> or UV light,<sup>30–35</sup> to form crosslinks. The presence of numerous reactive LA chain ends affords crosslinked networks with diverse physical properties. Finally, the redox-active disulfides in these bottlebrush networks present a unique opportunity to selectively degrade the materials electrochemically and regenerate the starting bottlebrush polymers. More reductive conditions can also be used, resulting in the complete degradation of ester-based side-chains and the disulfide crosslinks, for example,  $M_n = 2200 \text{ kg mol}^{-1} \rightarrow 1 \text{ kg mol}^{-1}$ . In summary, this is a simple and versatile synthetic platform for the preparation of degradable bottlebrush-based materials under mild conditions.

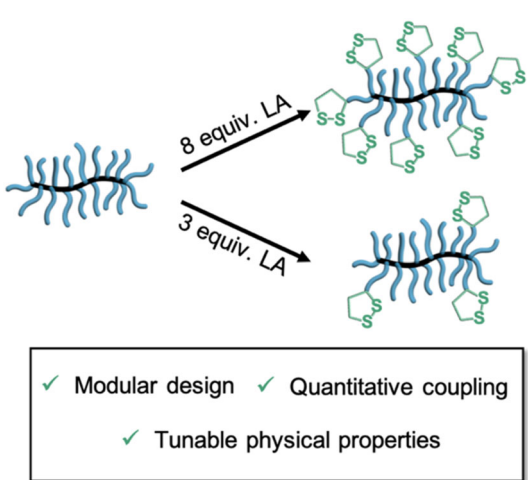


FIGURE 1 Highly tunable bottlebrush polymers functionalized with  $\alpha$ -lipoic acid (LA).

## 1.1 | Design and synthesis

A number of synthetic strategies are available for the controlled preparation of bottlebrush polymers. This includes grafting-from, grafting-to and grafting-through. For this study we selected grafting-through polymerization as the method of choice since it allows for the rigorous characterization of macromonomers prior to bottlebrush formation. Poly(4-methylcaprolactone) (P4MCL) was selected as the bottlebrush side-chain chemistry since (i) it is an amorphous polymer with a low glass transition temperature ( $T_g = -60^\circ\text{C}$ ), making it a suitable candidate for creating robust elastomers, (ii) extensive characterization and study has yielded insights into its (bio)degradability,<sup>36</sup> and (iii) the requisite ring-opening polymerization chemistry yields telechelic macromonomers that can be used for both bottlebrush formation and chain-end functionalization (see below). Telechelic P4MCL macromonomers (Table 1 and Figures S1–S4) were therefore synthesized via ring-opening polymerization (ROP) as previously reported in the literature starting from a norbornene alcohol initiator.<sup>21,37,38</sup> The resulting macromonomers contain a single norbornene end group suitable for ring-opening metathesis polymerization (ROMP) and a single hydroxyl chain end available for coupling to lipoic acid following bottlebrush formation.

P4MCL macromonomers with hydroxy chain ends were then used to synthesize bottlebrush polymers with targeted backbone degrees of polymerization ( $N_{BB}$ ) via ROMP with Grubbs third-generation bis-pyridine-based catalyst. In principle, larger values of  $N_{BB}$  yield softer networks, but as  $N_{BB}$  increases, bottlebrush-based materials become progressively more difficult to process.<sup>21</sup> For this reason, we targeted bottlebrush polymers with a moderate  $N_{BB}$  ( $\sim 200$ ) and macromonomers of varied side-chain degrees of polymerization ( $N_{SC}$ ) to yield a library of bottlebrush polymers. This highlights the tunability of the bottlebrush architecture and demonstrates the range of structures accessible with this platform.

We selected  $\alpha$ -lipoic acid (LA) as a crosslinker because of the facile dithiolane ring-opening under heat ( $\sim 70^\circ\text{C}$ ) or UV light ( $\sim 365 \text{ nm}$ ) with the pendant carboxylic acid on the LA serving as a convenient functional handle to couple with the numerous hydroxy chain ends of the P4MCL bottlebrush (Figure 2 and Figures S5–S7). To further complement the structural variations within the bottlebrush library, the number of crosslinkable LA chain ends can be tuned by controlling the degree of chain end functionalization. From the same bottlebrush polymer, functionalization with different equivalents of LA can be studied (Table 1) leading to networks with a range of crosslink densities from the same starting material. Note that this order

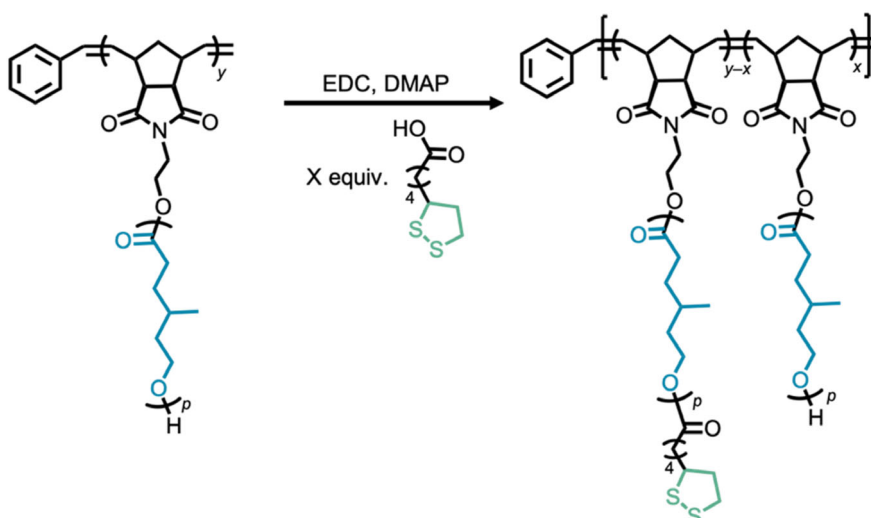
TABLE 1 Molecular characterization of  $\alpha$ -lipoic acid-functionalized bottlebrush polymers.

Bottlebrush	$N_{SC}^a$	$D^b$	$M_{n,BB}^b$	$N_{BB}^b$	$D^b$	LA equiv. (target)	LA equiv. (exper)
P4MCL <sup>14</sup> LA <sup>5</sup>	14	1.03	240	130	1.30	5	6.8
P4MCL <sup>14</sup> LA <sup>10</sup>	14	1.03	240	130	1.30	10	14
P4MCL <sup>14</sup> LA <sup>25</sup>	14	1.03	45	25	1.10	25	27

<sup>a</sup>Determined using end-group analysis via  $^1H$  NMR and reported in kg mol<sup>-1</sup>.

<sup>b</sup>Measured in multi-angle light scattering THF SEC analysis and reported in kg mol<sup>-1</sup>.

FIGURE 2 Synthesis of  $\alpha$ -lipoic acid functionalized bottlebrush polymers.



of operation—initial synthesis of the bottlebrush followed by functionalizing with LA—was necessary because directly functionalizing the macromonomer with LA followed by ROMP of the LA macromonomer resulted in presumed sulfur chelation to the ruthenium catalyst, rendering it inert.

## 1.2 | Characterization

First, we sought to precisely quantify the LA coupling efficiency to the bottlebrush polymer chain ends, which was challenging to characterize with traditional techniques (e.g.,  $^1H$  NMR and SEC) due to the insignificant molar mass of LA (0.2 kg mol<sup>-1</sup>) compared to the bottlebrush ( $\leq 2200$  kg mol<sup>-1</sup>). Taking advantage of the sensitivity of electrochemical analysis and the multiple redox-active disulfide bonds present in the LA chain ends, we hypothesized that electrochemistry would be a suitable method to determine the coupling efficiency of the esterification reaction. A series of bottlebrushes with varied molar masses and different target LA loadings were therefore probed (Table 1). First, we targeted quantitative (100%) functionalization of the side chains with LA ( $n \sim 25$  equiv. of LA per bottlebrush) for a 45 kg mol<sup>-1</sup> bottlebrush ( $N_{SC} = 14$ ,  $N_{BB} = 25$ , P4MCL<sup>14</sup> LA<sup>25</sup>). A small amount of the functionalized polymer was

dissolved in DMF with 0.1 M TBAPF<sub>6</sub> as an electrolyte (see the supporting information for a detailed procedure). Cyclic voltammograms (CV) were measured from 10 to 250 mV s<sup>-1</sup> (Figure 3A) showing an irreversible reduction peak at  $-2.54$  V versus ferrocene (Fc) with a linear increase in magnitude versus scan rate. The observed reduction peak matches the CV of LA bottlebrush P4MCL<sup>14</sup> LA<sup>25</sup> (Figure S27a) and is attributed to reduction of the S–S bond.<sup>39,40</sup> As the peak current increased linearly with the square root of scan rate, the concentration of LA per bottlebrush was determined using the Randles–Sevcik equation (Equation (S2)), where the measured equivalents of LA groups ( $n \sim 27$ ) is in good agreement with the targeted value ( $n = 25$ , see Figure S28). This measurement was repeated with a 240 kg mol<sup>-1</sup> bottlebrush (bottlebrushes P4MCL<sup>14</sup> LA<sup>5</sup> and P4MCL<sup>14</sup> LA<sup>10</sup>) at various loadings of LA (Figures S29 and S30). In all cases, the calculated level of functionalization matched closely to the theoretical LA target, indicating essentially 100% coupling efficiency was achieved in the presence of EDC and DMAP (Figure 3B). Over-estimated values obtained by this method can be attributed to the error of the measurement and the dispersity of the bottlebrush polymers ( $N_{BB}$  and  $N_{SC}$ ).

Next, we investigated the curing kinetics of a LA bottlebrush with  $N_{SC} = 47$ ,  $N_{BB} = 350$ , and an average of

6 LA groups at the chain ends of the bottlebrush by monitoring the change in shear modulus via rheology. After irradiating with 365 nm light for 45 min at 400 mW/cm<sup>2</sup>, network formation was observed as evidenced by a plateau in the storage modulus ( $G'$ ). To improve the curing kinetics at lower UV intensities, phenylbis(2,4,6-trimethylbenzoyl)phosphine oxide (BAPO) (2 wt %) was added as a radical initiator to the formulation (Figure S15) which enhanced network formation and allows the system to be fully cured within 1–3 min of irradiation at 50 mW/cm<sup>2</sup>. With accessible kinetics in hand, we synthesized a series of 2100 kg mol<sup>-1</sup> bottlebrush polymers ( $N_{SC} = 47$ ,  $N_{BB} = 350$ ) with LA functionalization levels of ~6, 12, and 20 groups per bottlebrush polymer. As expected, increasing the level of LA

functionalization yielded a stiffer elastomer ( $n \sim 20$  LA,  $G' = 24$  kPa) compared to the network with fewer cross-links ( $n \sim 3$  LA,  $G' = 8$  kPa) (Figure 4). Macroscopically this results in the network based on a bottlebrush with 20 LA functional groups at the chain ends being a stretchable elastomer whereas the network formed from the bottlebrush with 3 LA functional groups resulted in a material reminiscent of an adhesive (Figure 4 and Figures S17–22).

### 1.3 | Degradation

The disulfide crosslinks formed after ring-opening of the LA chain ends present a unique opportunity for selective

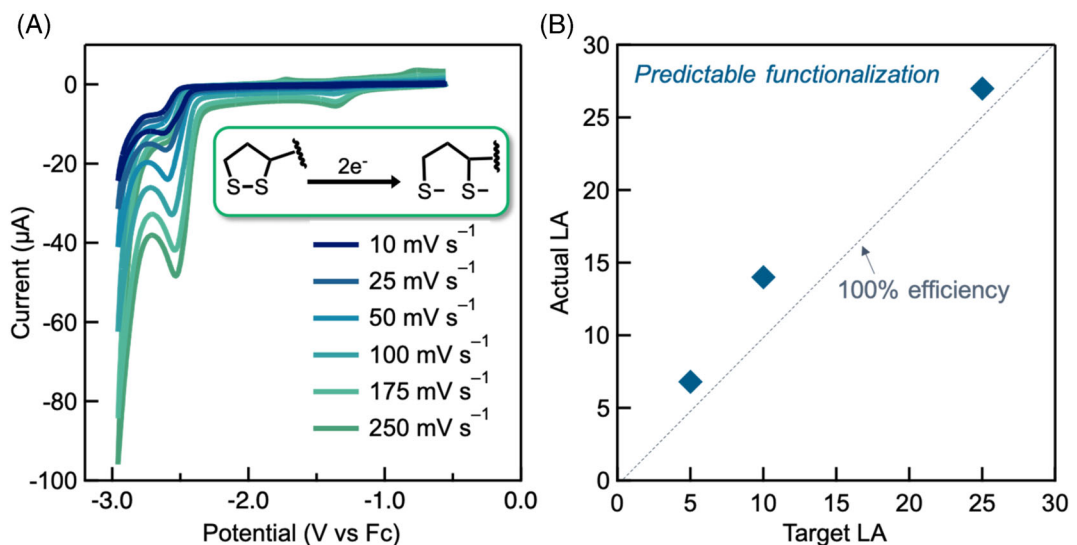


**FIGURE 3** Quantifying  $\alpha$ -lipoic acid incorporation from redox-active disulfides. (A) Cyclic voltammograms show an irreversible reduction peak of P4MCL<sup>14</sup> LA<sup>25</sup> at  $-2.54$  V versus Fc associated with reduction of the S–S bond. These measurements were used to quantify (B) the level of LA chain end functionalization versus the theoretical level of functionalization assuming quantitative coupling.

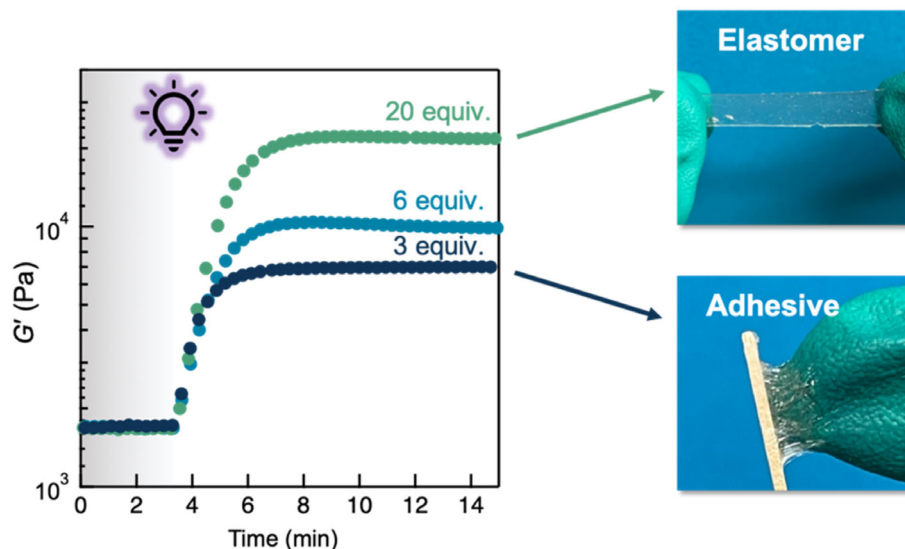
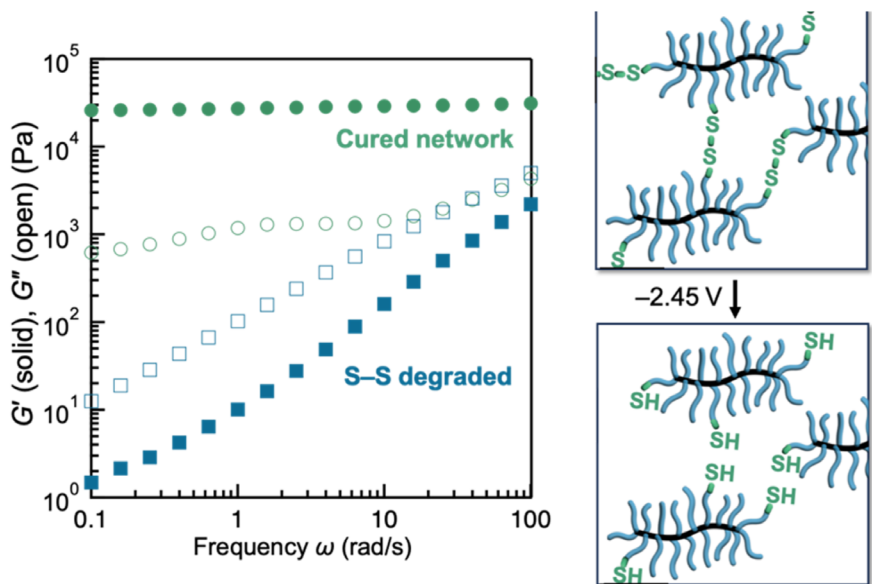


**FIGURE 4** Kinetics of bottlebrush network formation with different levels of  $\alpha$ -lipoic acid functionalization. UV light was turned on after 200 s. Networks formed from bottlebrushes with 20 LA groups at the chain ends gives stretchable elastomers (top) while the same bottlebrush functionalized with 3 LA groups results in a high-strength adhesive (bottom). Bottlebrush networks were formed in the presence of BAPO as a photoinitiator.

**FIGURE 5** Bottlebrush networks crosslinked with  $\alpha$ -lipoic acid are selectively degraded through electrochemical reduction of the disulfide bonds. This degradation is evident by frequency sweeps performed on the cured bottlebrush network before (viscoelastic solid) and after (viscoelastic liquid) electrochemical degradation.



and mild degradation of the bottlebrush network. This is driven by the dynamic nature of disulfide bonds which are responsive to electrochemistry and mild reducing agents. To test the degradability of these bottlebrush networks, a  $2100 \text{ kg mol}^{-1}$  bottlebrush ( $N_{\text{SC}} = 47$ ,  $N_{\text{BB}} = 350$ ,  $n \sim 20$  LA units) was cured with UV light on a working electrode and submersed in a solution of  $\text{LiClO}_4$  in DMF. After 4 h, at a constant voltage of  $-2.54 \text{ V}$ , the network had completely dissolved in the DMF solution (Figure S23). The polymer remaining after electrochemical reduction was dried and characterized via SEC. The SEC trace of the degraded bottlebrush exhibited a similar molar mass distribution as the LA-functionalized bottlebrush prior to initial crosslinking (Figure S24). Rheology was used to confirm network degradation with the loss modulus ( $G''$ ) dominating the storage modulus ( $G'$ ) signifying that the degraded material is a viscoelastic liquid (Figure 5). Similar results were obtained through chemical reduction of the disulfide bonds using tris(2-carboxyethyl)phosphine (TCEP) as a mild chemical reducing agent (Figures S25 and S26) at  $60^\circ\text{C}$  after 16 h.

In addition, both the ester groups in the P4MCL side-chains and the S–S crosslinks can be degraded simultaneously utilizing more reactive chemical reducing conditions. To test full degradability, a cured sample was placed in a solution of tetrahydrofuran (THF) and allowed to react with sodium borohydride ( $\text{NaBH}_4$ ) with complete degradation being observed after 12 h. In contrast, a cured sample suspended in pure THF at  $50^\circ\text{C}$  only resulted in a swollen network with minimal or no observed degradation. SEC also supports complete degradation (network and side chains) with the bottlebrush molar mass being reduced from  $2100$  to  $\sim 1 \text{ kg mol}^{-1}$  (Figure S31).

## 2 | CONCLUSIONS

In conclusion, this work demonstrates that  $\alpha$ -lipoic acid is a versatile crosslinker for highly tunable bottlebrush networks. The numerous hydroxyl termini of P4MCL side chains provide a synthetic handle to controllably install LA residues with a range of loading levels which in turn can be used to tune the physical and mechanical properties of the network. The chemical versatility of the LA chain ends allows for crosslinking under thermal or photochemical conditions through ring-opening of the dithiolane ring. The resulting disulfide crosslinks enables selective electrochemical degradation of the bottlebrush network to regenerate the starting bottlebrush polymer. Additionally, complete degradation of both the polyester side chains and disulfides was achieved using harsher reducing conditions. This platform represents a simple strategy for synthesizing highly tunable and degradable bottlebrush elastomers.

## ACKNOWLEDGMENTS

This work was supported by the BioPACIFIC Materials Innovation Platform of the National Science Foundation under Award No. DMR-1933487. The research reported here made use of shared facilities of the UC Santa Barbara Materials Research Science and Engineering Center (MRSEC, NSF DMR-2308708), a member of the Materials Research Facilities Network (<http://www.mrfn.org>).

## ORCID

Christopher M. Bates  <https://orcid.org/0000-0002-1598-794X>

## REFERENCES

[1] M. Vatankhah-Varnoosfaderani, W. F. M. Daniel, A. P. Zhushma, Q. Li, B. J. Morgan, K. Matyjaszewski, D. P. Armstrong, R. J. Spontak, A. V. Dobrynnin, S. S. Sheiko, *Adv. Mater.* **2017**, *29*, 1604209.

[2] S. Mukherjee, R. Xie, V. G. Reynolds, T. Uchiyama, A. E. Levi, E. Valois, H. Wang, M. L. Chabiny, C. M. Bates, *Macromolecules* **2020**, *53*, 1090.

[3] V. G. Reynolds, S. Mukherjee, R. Xie, A. E. Levi, A. Atassi, T. Uchiyama, H. Wang, M. L. Chabiny, C. M. Bates, *Mater. Horiz.* **2020**, *7*, 181.

[4] J. L. Self, C. S. Sample, A. E. Levi, K. Li, R. Xie, J. R. De Alaniz, C. M. Bates, *J. Am. Chem. Soc.* **2020**, *142*, 7567.

[5] W. F. M. Daniel, J. Burdyńska, M. Vatankhah-Varnoosfaderani, K. Matyjaszewski, J. Paturej, M. Rubinstein, A. V. Dobrynnin, S. S. Sheiko, *Nat. Mater.* **2016**, *15*, 183.

[6] L.-H. Cai, T. E. Kodger, R. E. Guerra, A. F. Pegoraro, M. Rubinstein, D. A. Weitz, *Adv. Mater.* **2015**, *27*, 5132.

[7] C. Choi, J. L. Self, Y. Okayama, A. E. Levi, M. Gerst, J. C. Speros, C. J. Hawker, J. Read de Alaniz, C. M. Bates, *J. Am. Chem. Soc.* **2021**, *143*, 9866.

[8] G. Xie, M. R. Martinez, M. Olszewski, S. S. Sheiko, K. Matyjaszewski, *Biomacromolecules* **2019**, *20*, 27.

[9] M. Müllner, A. H. E. Müller, *Polymer* **2016**, *98*, 389.

[10] S. S. Sheiko, B. S. Sumerlin, K. Matyjaszewski, *Prog. Polym. Sci.* **2008**, *33*, 759.

[11] H. Lee, J. Pietrasik, S. S. Sheiko, K. Matyjaszewski, *Prog. Polym. Sci.* **2010**, *35*, 24.

[12] J. Rzayev, *ACS Macro Lett.* **2012**, *1*, 1146.

[13] S. Zheng, H. Xue, J. Yao, Y. Chen, M. A. Brook, M. E. Noman, Z. Cao, *ACS Appl. Mater. Interfaces* **2023**, *15*, 41043.

[14] B. Sieredzinska, Q. Zhang, K. J. V. D. Berg, J. Flapper, B. L. Feringa, *Chem. Commun.* **2021**, *57*, 9838.

[15] M. R. Martinez, S. Dadashi-Silab, F. Lorandi, Y. Zhao, K. Matyjaszewski, *Macromolecules* **2021**, *54*, 5526.

[16] K. J. Arrington, S. C. Radzinski, K. J. Drumme, T. E. Long, J. B. Matson, *ACS Appl. Mater. Interfaces* **2018**, *10*, 26662.

[17] Q. Un Nisa, W. Theobald, K. S. Hepburn, I. Riddlestone, N. M. Bingham, M. Kopeć, P. J. Roth, *Macromolecules* **2022**, *55*, 7392.

[18] W. Raj, K. Jerczynski, M. Rahimi, A. Przekora, K. Matyjaszewski, J. Pietrasik, *Mater. Sci. Eng. C* **2021**, *130*, 112439.

[19] C. Riachi, N. Schüwer, H.-A. Klok, *Macromolecules* **2009**, *42*, 8076.

[20] V. Delplace, A. Tardy, S. Harrisson, S. Mura, D. Gigmès, Y. Guillaneuf, J. Nicolas, *Biomacromolecules* **2013**, *14*, 3769.

[21] J. L. Self, V. G. Reynolds, J. Blankenship, E. Mee, J. Guo, K. Albanese, R. Xie, C. J. Hawker, J. R. De Alaniz, M. L. Chabiny, C. M. Bates, *ACS Polym. Au* **2022**, *2*, 27.

[22] H. Mei, A. H. Mah, Z. Hu, Y. Li, T. Terlier, G. E. Stein, R. Verduzco, *ACS Macro Lett.* **2020**, *9*, 1135.

[23] K. R. Albanese, J. Read de Alaniz, C. J. Hawker, C. M. Bates, *Polymer* **2024**, *304*, 127167.

[24] K. R. Albanese, P. T. Morris, J. Read de Alaniz, C. M. Bates, C. J. Hawker, *J. Am. Chem. Soc.* **2023**, *145*, 22728.

[25] K. Endo, T. Yamanaka, *Macromolecules* **2006**, *39*, 4038.

[26] A. Kisanuki, Y. Kimpara, Y. Oikado, N. Kado, M. Matsumoto, K. Endo, *J. Polym. Sci. Part Polym. Chem.* **2010**, *48*, 5247.

[27] R. C. Thomas, L. J. Reed, *J. Am. Chem. Soc.* **1956**, *78*, 6148.

[28] Q. Zhang, C.-Y. Shi, D.-H. Qu, Y.-T. Long, B. L. Feringa, H. Tian, *Sci. Adv.* **2018**, *4*, eaat8192.

[29] C. Dang, M. Wang, J. Yu, Y. Chen, S. Zhou, X. Feng, D. Liu, H. Qi, *Adv. Funct. Mater.* **2019**, *29*, 1902467.

[30] G. M. Scheutz, J. L. Rowell, S. T. Ellison, J. B. Garrison, B. S. Sumerlin, *Macromolecules* **2020**, *53*, 4038.

[31] P. R. Brown, J. O. Edwards, *J. Org. Chem.* **1969**, *34*, 3131.

[32] M. A. Alraddadi, V. Chiaradia, C. J. Stubbs, J. C. Worch, A. P. Dove, *Polym. Chem.* **2021**, *12*, 5796.

[33] Q. Zhang, D.-H. Qu, B. L. Feringa, H. Tian, *J. Am. Chem. Soc.* **2022**, *144*, 2022.

[34] B.-S. Wang, D.-H. Qu, *Chem. Lett.* **2023**, *52*, 496.

[35] K. R. Albanese, Y. Okayama, P. T. Morris, M. Gerst, R. Gupta, J. C. Speros, C. J. Hawker, C. Choi, J. R. Read de Alaniz, C. M. Bates, *ACS Macro Lett.* **2023**, *12*, 787.

[36] D. C. Batiste, G. X. De Hoe, T. F. Nelson, K. Sodnikar, K. McNeill, M. Sander, M. A. Hillmyer, *ACS Sustainable Chem. Eng.* **2022**, *10*, 1373.

[37] R. Xie, I. Lapkriengkri, N. B. Pramanik, S. Mukherjee, J. R. Blankenship, K. Albanese, H. Wang, M. L. Chabiny, C. M. Bates, *Macromolecules* **2022**, *55*, 10513.

[38] A. Watts, N. Kurokawa, M. A. Hillmyer, *Biomacromolecules* **2017**, *18*, 1845.

[39] J. K. Howie, J. J. Houts, D. T. Sawyer, *J. Am. Chem. Soc.* **1977**, *99*, 6323.

[40] J. M. M. Pople, T. P. Nicholls, L. N. Pham, W. M. Bloch, L. S. Lisboa, M. V. Perkins, C. T. Gibson, M. L. Coote, Z. Jia, J. Chalker, *J. Am. Chem. Soc.* **2023**, *145*, jacs.3c03239.

## SUPPORTING INFORMATION

Additional supporting information can be found online in the Supporting Information section at the end of this article.

**How to cite this article:** K. R. Albanese, P. T. Morris, B. Roehrich, J. Read de Alaniz, C. J. Hawker, C. M. Bates, *J. Polym. Sci.* **2024**, *1*, <https://doi.org/10.1002/pol.20240393>